COMPOSITE FERMION THEORY OF FRACTIONAL QUANTUM HALL EFFECT*

J.K. JAIN

Department of Physics, State University of New York at Stony Brook
Stony Brook, New York 11794-3800, USA

(Received November 2, 1995)

Composite fermion, which is an electron carrying an even number of vortices of the many body wave function, is a new kind of topological particle, formed in a range of parameters when electrons in two dimensions are subjected to a strong magnetic field. The composite fermions have the same charge and statistics as electrons, but differ from electrons in the important respect that they experience a drastically reduced magnetic field. This article gives an elementary introduction to composite fermions and describes how they help gain a simple understanding of the dramatic phenomena exhibited by two-dimensional electrons in high magnetic fields. It is based on lectures given at the "XXXV Jubilee Cracow School of Theoretical Physics" in Zakopane, Poland.

PACS numbers: 73.40.Hm

1. Introduction

The first task in approaching any problem in physics is to decide what variable to use in the formulation of the problem. This issue is of primary importance, since the physics can appear extremely complicated in terms of one set of variables yet delightfully simple in another. In general, the objective is to find a set of variables which are 'weakly coupled', *i.e.*, the qualitative physics is well described even if the interaction between these variables is completely neglected. These will be called the relevant particles of the problem. Once this is accomplished, an effectively single particle description of the qualitative features of the system in question becomes possible.

---

* Presented at the XXXV Cracow School of Theoretical Physics, Zakopane, Poland, June 4–14, 1995.

The choice of the relevant particles is usually made by a close inspection of experiments. We confine our discussion below to condensed matter systems. Perhaps the simplest example is that of lattice vibrations. A neglect the coupling between different atoms (the Einstein model) will produce incorrect low-energy spectrum and low-temperature specific heat. The appropriate set of variables are the normal modes, *i.e.*, the phonons, which can be taken as non-interacting to a good first approximation. Same is true for single spin flips *versus* magnons (spin waves). Both the phonons and magnons can be obtained by diagonalizing simple Hamiltonians with nearest neighbor couplings.

In electronic systems, the relevant variables are not so obvious, at least in the beginning, and can usually not be obtained rigorously by solving a Hamiltonian. Here, one essentially postulates their existence based on experiments, and then tests the consequences both theoretically and experimentally. The best known example is that of interacting electrons in a normal conductor. At one time, it was a mystery why the noninteracting model worked so well here. Landau explained that the noninteracting objects are not really electrons, but entities similar to electrons, called "Landau quatiparticles". *I.e.,* the interacting electrons resemble weakly interacting Landau quasiparticles. In this instance, the relevant particles turn out to be qualitatively similar (and perturbatively connected) to electrons, but this need not be the case in general. A superconductor is, for example, described in terms of a weakly interacting gas of charge-$2e$ boson-like Cooper pairs. In fact, one can designate as 'strongly correlated' those systems in which the 'output' particles, *i.e.*, the particles in terms of which the physics is described *most simply*, are *qualitatively* different from the 'input' particles, which appeared in the definition of the problem.

Here we consider the problem of interacting electrons in two dimensions exposed to a strong magnetic field. In this case, the kinetic degree of freedom is quenched, and all of the physics arises from the interelectron interaction. There is no small parameter here; the interaction is not small compared to any other energy scale in the problem, for the simple reason that no other relevant energy scale exists. A perturbative treatment of the interaction, like that in Landau's Fermi liquid theory, is therefore not possible. At the first glance, one might feel that the problem is hopelessly complicated. This system, however, exhibits remarkably simple behavior, strongly suggesting that a simple description of the relevant physics ought to be possible. Recent developments have shown that this is indeed the case. The strongly correlated liquid of electrons is well described in terms of a weakly interacting gas of a new type of particles, called "composite fermions". The composite fermions have the same quantum number as electrons, but are qualitatively distinct from the electrons in their property that they experience a much

reduced electromagnetic field. The purpose of this article is to provide an introduction to composite fermions, discuss how they explain several experimental facts quite straightforwardly, and describe the comparison of the composite fermion theory with the exact theoretical calculations. Only the essential results will be given here in some detail.

2. Phenomenology of quantum Hall effect

Two-dimensional electrons display quantum Hall effect (QHE) when subjected to an intense transverse magnetic field. The Hall resistance [1] has plateaus at the quantized values

$$R_H = \frac{h}{fe^2}, \tag{1}$$

where f is either an integer [2], or a simple rational fraction [3]. The former is called the integer QHE (IQHE) and the latter the fractional QHE (FQHE). The prominent fractions appear in certain sequences, some of which are:

$$f = n = 1,\ 2,\ 3,\ \ldots, \quad f = \frac{n}{2n+1} = \frac{1}{3},\ \frac{2}{5},\ \frac{3}{7},\ \ldots,$$

$$f = \frac{n}{2n-1} = \frac{2}{3},\ \frac{3}{5},\ \frac{4}{7},\ \ldots, \quad f = \frac{n}{4n+1} = \frac{1}{5},\ \frac{2}{9},\ \frac{3}{13},\ \ldots,$$

$$f = \frac{n}{4n-1} = \frac{2}{7},\ \frac{3}{11},\ \frac{4}{15},\ \ldots.$$

All observed fractions with $f < 1$ have odd-denominators. The longitudinal resistance in the plateau region vanishes exponentially with temperature. Fig. 1 shows the QHE in its full splendor [4].

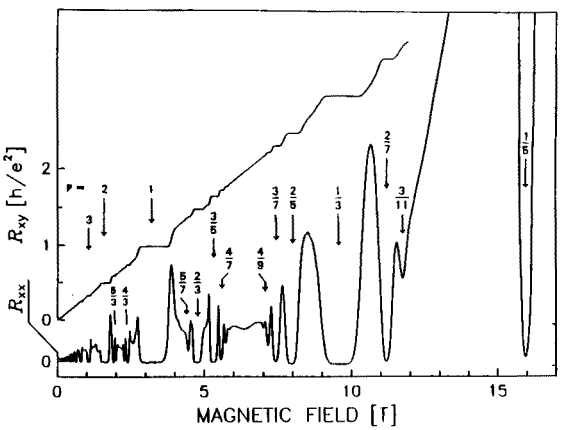

Fig. 1. A plot of the Hall and the longitudinal resistances, R_{xy} and R_{xx}. Source: Ref. [4], with permission.

3. Composite fermions

Prior to the CF theory, the FQHE and the IQHE were treated as two distinct phenomena, and there was no satisfactory overall understanding of the FQHE. (For a review of the pre-composite fermion theories, see Ref. [5]). The concept of composite fermions was originally postulated in order to provide a unified description of the QHE, in which the FQHE of electrons is equivalent to the IQHE of composite fermions [6].

We will assume below, unless explicitly stated otherwise, that the magnetic field is sufficiently large to polarize all electrons. In other words, we will consider spinless particles (both electrons and composite fermions).

A composite fermion is an electron carrying an even number ($2m$) of vortices of the many-electron wave function. It is a collective quantum-mechanical object, but behaves nonetheless like a particle. Its fundamental defining properties are: (a) It has the same quantum numbers as an electron, *i.e.*, charge $-e$ and spin 1/2. (b) It obeys fermionic statistics. (c) It experiences an effective magnetic field

$$B^* = B - 2m\rho\phi_0\,, \tag{2}$$

where B is the external magnetic field (as experienced by the electrons), ρ is the (area) density of electrons (or composite fermions), and $\phi_0 = hc/e$ is the quantum of flux. (d) In the presence of an applied electric field, E, composite fermions also experience an effective electric field, E^*, given by [7]

$$\frac{E^*}{B^*} = \frac{E}{B}\,. \tag{3}$$

The origin of the first two properties is obvious, since the composite fermion is nothing but a screened electron. The property (c), which differentiates a composite fermion from an electron, follows from the feature that the screening occurs in a very special way, through a dressing of each electron by an even number of vortices (converting it into a composite fermion). As the composite fermions move around, the vortices bound to them produce extra phases, which partly cancel the Aharonov–Bohm phases produced by the external field. It therefore seems as though the composite fermion were moving in a reduced effective magnetic field. In order to compute this field, take a composite fermion around a closed loop of area A. The Aharonov-Bohm phase associated with this path is $2\pi AB/\phi_0$. There are ρA composite fermions inside the loop with a total of $2m\rho A$ vortices bound to them. Since each vortex gives a phase -2π, the net phase from the vortices is $-4m\pi\rho A$. Equating the total phase to $2\pi AB^*/\phi_0$ gives the above formula for B^*. The renormalization of the electric field can be seen as follows [7]. For a crossed electric and magnetic field, the magnitude of the current density in

a translationally invariant system is $\rho ev = \rho ecE/B$, since the electric field, and consequently the current is zero in a frame of reference moving with a velocity $v = cE/B$ (in a direction perpendicular to the plane containing the electric and magnetic fields). This result is general, independent of the interelectron interactions, implying that the current is the same for composite fermions as for electrons. Consequently, the electric field experienced by the composite fermions must be renormalized according to the above equation. In effect, while the cyclotron orbit of a composite fermion is determined by B^*, its drift velocity is the same as that of an electron.

The "intrinsic" charge of the composite fermion, which determines its coupling to the external electromagnetic field, is universally $-e$, as used in the derivation of Eq. (2). Another important quantum number is the "local charge" of the composite fermion [7], which is equal to its intrinsic charge plus the charge of the screening cloud. It is not listed as one of the fundamental properties of the composite fermion, since *(i)* it is not always sharply defined, and *(ii)* its value depends on the screening properties of the background CF state. The local charge of a composite fermion residing on the background of the n filled CF-Landau levels is quantized, given by $|e^*| = e/(2mn \pm 1)$, as can be shown by a simple counting argument [8, 7]. Thus, in a sense, the dielectric constant of an incompressible CF state is quantized. For a composite fermion in a *compressible* CF state, the local charge is not a sharp observable (even though the intrinsic charge is).

In the presence of a transverse magnetic field, electrons form Landau levels (LL's) [9], with the degeneracy per LL per unit area given by Be/hc. The nominal number of filled LL's, called the filling factor, is

$$\nu = \frac{\rho\phi_0}{B} . \tag{4}$$

The composite fermions are formed approximately in the filling factor range $1 > \nu > 1/5$ in the lowest LL, and also in certain smaller ranges of filling factors greater than unity. (For very small fillings, $\nu < 1/5$, the lowest energy state is a Wigner crystal.) The composite fermions form LL's in the reduced magnetic field B^*, which will be called CF-LL's to distinguish them from the electron LL's. (Note that the composite fermions can fill several CF-LL's even when electrons are confined to *their* lowest LL.) Noting that B^* can be either positive or negative, the CF filling factor is given by

$$\nu^* = \frac{\rho\phi_0}{|B^*|} . \tag{5}$$

Eq. (2) can be expressed as a relation between ν and ν^*:

$$\nu = \frac{|\nu^*|}{2m|\nu^*| \pm 1} , \tag{6}$$

where the + (−) sign corresponds to positive (negative) B^*.

The composite fermions are generated dynamically as a result of the repulsive Coulomb interaction between electrons. This will become clearer in a later section, when we write the wave functions of composite fermion states, which illustrate how binding of vortices to electrons helps them stay away from one another. The wave functions will also clarify why a binding of an *odd* integer number of vortices is not allowed, due to the requirement of antisymmetry of the electronic wave function.

It is often intuitively useful, though not literally correct, to view the composite fermion as an electron carrying an even number of flux quanta; this model produces the correct phases as the composite fermions move around. In this picture, electrons absorb part of the external magnetic flux to become composite fermions, which then move in the weaker residual magnetic field.

Without much further ado, we now show how the CF hypothesis provides back-of-the-envelope explanations of a large number of experimental facts, confirming that the composite fermions are indeed the elementary particles of the FQHE.

4. Experimental evidence for composite fermions

4.1. FQHE

The CF theory produces a simple understanding of the FQHE. Let us first state, without proof, the conditions for the QHE [10]. A quantized Hall plateau at $R_H = h/fe^2$ is obtained if a sufficiently weak disorder is introduced in a system which has a gap in the excitation spectrum at $\nu = f$ in the absence of disorder. For noninteracting electrons, there is a gap in the excitation spectrum when the system consists of an integer number of filled LL's, *i.e.*, when $\nu = n$. This results in the IQHE. No other quantized plateaus are possible for noninteracting electrons.

In the lowest LL of electrons, we assume that composite fermions are formed, with their filling factor given by ν^*. A gap appears whenever composite fermions fill an integer number of CF-LL's. Filled CF-LL's of composite fermions correspond to electron filling factors of

$$f = \frac{n}{2mn \pm 1}. \tag{7}$$

These, along with the states $f = 1 - (n/2mn \pm 1)$, related by particle-hole symmetry in the lowest LL (LLL), are called the principal fractions, and produce the sequences of observed fractions. The FQHE of electrons is thus simply the IQHE of composite fermions. Note that only odd-denominator fractions are obtained, in agreement with experiments.

4.2. Transitions between plateaus

At the transition from one FQHE state to the next, the Hall resistance jumps from one plateau to another, and the longitudinal resistance exhibits a peak. In the CF theory, this transition is simply the transition between $f^* = n$ IQHE of composite fermions to $f^* = n + 1$ IQHE [11]. For low-disorder samples, it is expected to occur when the CF-Fermi level passes through the extended states, which happens (in the simplest scenario) at $\nu^* = n + 1/2$. This corresponds to the electron filling factor $\nu = (2n + 1)/[2m(2n + 1) + 2]$. This prediction has been found to be in excellent agreement with the experimental positions of the longitudinal resistance peaks [12]. Engel *et al.* [13] have found that the temperature dependence of the width of the transition region is characterized by the same exponent in the FQHE regime as in the IQHE regime, which is also naturally explainable within the CF framework [11]. Recently, Rokhinson *et al.* [14] have investigated the conductivity peak heights in the FQHE regime, and confirmed their relation with the peak heights in the IQHE regime, derived in Ref. [15]. The knowledge of peak positions also tells us the widths of various plateaus in low-disorder samples.

4.3. Gaps

An important experimentally measurable quantity is the gap of a FQHE state. As we will see, the CF theory gives accurate wave functions for the ground and the excited states, and therefore, can, in principle, provide reasonable estimates for the gaps in the small disorder limit. Bonesteel [16] has computed the gap for the 1/3 state using the CF wave functions, which agrees well with that obtained by other means [17]. However, for technical reasons, a computation of the gaps of the other FQHE states has proven to be a formidable task.

Halperin, Lee, and Read [18] have suggested a simple picture in which the gap of a FQHE state is viewed as the cyclotron energy of the composite fermions. The gap of the $n/(2mn \pm 1)$ state is

$$\hbar\omega_c^* = \hbar\frac{eB^*}{m^*c}, \tag{8}$$

where m^* is the effective mass of the composite fermion, and $\hbar\omega_c^*$ is the CF-cyclotron energy. Du *et al.* [19] determined the gaps of five members of the principal sequences for two different samples and found that they are well approximated by $\hbar\omega_c^* - \Gamma$, where Γ is a constant. This fits nicely with the above prediction, provided Γ is interpreted [19] as the disorder-induced broadening of the CF-LL's. The effective mass estimated from these

experiments is roughly an order of magnitude larger than the band mass of the electron in GaAs.

4.4. Shubnikov–de Haas oscillations

Leadley *et al.* and Du *et al.* [20] have successfully analyzed the minima and maxima around $\nu = 1/2$ in terms of the Shubnikov–de Haas oscillations of composite fermions, in analogy to the Shubnikov–de Haas oscillations of electrons near $B = 0$. This also allows a determination of the effective mass of composite fermions, which is in general agreement with the mass obtained from the gap measurements.

4.5. Fermi sea of composite fermions

Even though there is no kinetic energy in the problem of interacting electrons in the LLL, the interaction energy between electrons effectively acts as the kinetic energy of composite fermions, as evidenced by the formation of the LL's of composite fermions. A limiting case, with $B^* = 0$ or $\nu^* = \infty$, corresponds to $\nu = 1/2m$. Provided the CF description continues to be valid here, composite fermions will fill an infinite number of CF-LL's, or, in other words, form a Fermi sea. Halperin, Lee and Read [18] (also see Kalmeyer and Zhang [21]) investigated the Fermi sea at $\nu = 1/2$ theoretically and concluded that it is stable and has a sharp Fermi surface. It is analogous to the Fermi sea of electrons at $B = 0$, with the difference that the composite fermions at $B^* = 0$ are fully spin-polarized, while the electrons at $B = 0$ are spin-unpolarized. As a result, the Fermi wave vector of composite fermions is $k_F^* = \sqrt{2}\, k_F$, where k_F is the Fermi wave vector of electrons at $B = 0$.

Three recent experiments [22–24] have confirmed the existence of composite fermions in the compressible region near $B^* = 0$ (that is, near $B = 2\rho\phi_0$) by observing the cyclotron motion of composite fermions at small B^*. As the magnetic field is moved slightly away from $B^* = 0$, composite fermions are expected to execute a cyclotron orbit with radius

$$R^* = \hbar \frac{k_F^*}{eB^*} . \tag{9}$$

Since $k_F^* = \sqrt{2} k_F$, the cyclotron radius of composite fermions at B^* is equal to that of electrons at $B = B^*/\sqrt{2}$, so that the structures near $B = 0$ and $B^* = 0$ should look similar provided they are plotted on scales differing by a factor of $\sqrt{2}$. The experiments in [22] and [23] are based on rather simple ideas. Goldman *et al.* [22] observe magnetic focusing of composite fermions near $\nu = 1/2$. The experimental set-up is shown in Fig. 2; the

current flows from 1 to 2, and the voltage is measured between 3 and 4. Near $B = 0$, a number of quasiperiodic peaks are observed (lower panel of Fig. 2), which occur at those values of B where the electrons coming straight out of the left constriction are focused into the right constriction, possibly after several specular reflections from the gate. Similar quasiperiodic structure was observed near $B^* = 0$ (upper panel). Kang *et al.* [23] study transport in antidot superlattices. The resistances near $B = 0$ and $B^* = 0$ are shown in Fig. 3. Near $B = 0$, peaks in the resistance occur when the cyclotron orbit is commensurate with the lattice; some of the most relevant commensurate orbits are shown in the figure. Similar dimensional resonances of composite fermions show up near $B^* = 0$. A close correspondence between the electron and the composite fermion peaks is evident in both Figs 2 and 3.

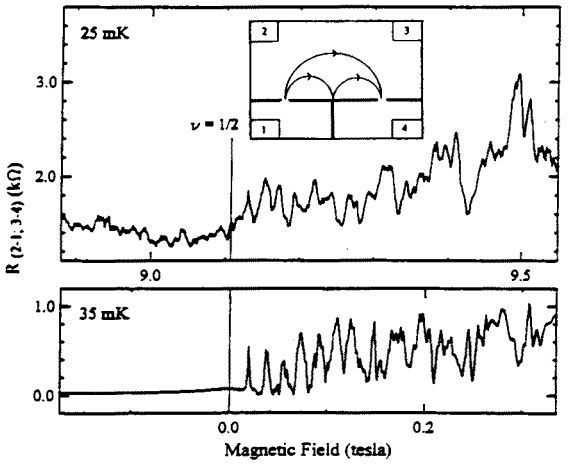

Fig. 2. The resistance $R_{(2-1;3-4)} = V_{34}/I_{21}$ for the magnetic focusing sample shown in the inset. The lower trace shows focusing peaks of electrons near $B = 0$, and the upper trace shows focusing peaks of composite fermions near $B^* = 0$ (that is, near $\nu = 1/2$). The B and B^* scales differ approximately by a factor of $\sqrt{2}$. A qualitative difference between the positive and negative B^* (that is, between $\nu > 1/2$ and $\nu < 1/2$) is evident, as is the one-to-one correspondence between several composite fermion and electron focusing peaks. Source: Ref. [22].

These experiments lead to the following conclusions: *(i)* Composite fermions exist in the region near $\nu = 1/2$, as follows from the fact that the cyclotron dynamics of the charge carriers is described by the effective

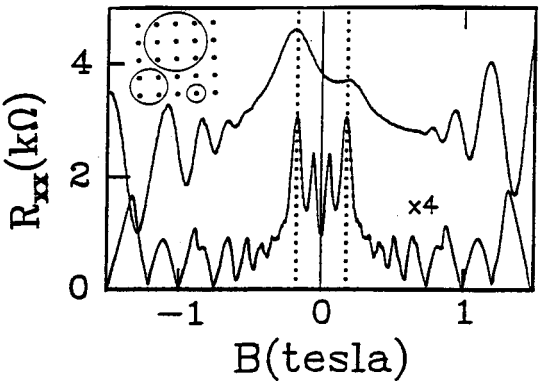

Fig. 3. The resistance of an antidot superlattice, shown in the inset, in the vicinity of $B = 0$ (lower curve) and $B^* = 0$ (upper curve). The scales for B and B^* differ by a factor of $\sqrt{2}$. The vertical dotted lines show the peaks corresponding to the smallest commensurate cyclotron orbit, enclosing only one antidot (see inset). The composite fermion peaks for other cyclotron orbits (*e.g.*, those enclosing four or nine antidots) are not seen presumably because of the relatively small mean free path of composite fermions. Source: Ref. [23].

field B^* rather than the external field B. *(ii)* The intrinsic charge of the composite fermion is $-e$ (as determined from the cyclotron radius). *(iii)* The statistics of the composite fermions is fermionic, as indicated by the measurement of the Fermi wave vector. *(iv)* A quasiclassical description also applies to composite fermions. The quasiclassical cyclotron orbits of composite fermions are quantized at larger B^* to produce CF-LL's, resulting in the FQHE.

Finally, the fact that the Hall resistance of the composite fermions is the same as that of electrons can be understood in terms of an effective electric field; both B^* and E^* approach zero as $\nu \to 1/2$, but the ratio, which determines the current, remains equal to E/B. The renormalization of the electric field must be considered at other filling factors as well, to get the correct Hall resistance [25].

Other experiments near $\nu = 1/2$ have also been analyzed in terms of composite fermions. In particular, Ying *et al.* [26] have found that the thermopower can be understood nicely using the independent CF picture.

The CF theory thus provides a coherent account of experiments. Next we show that it also leads to a simple microscopic description.

5. Theoretical tests

Theoretically, the aim is to solve the quantum mechanical problem defined by the Hamiltonian

$$H = \frac{1}{2} \sum_{j \neq k} \frac{e^2}{r_{jk}}, \tag{10}$$

within the Hilbert space of the lowest LL. This Hamiltonian is obtained in the limit $B \to \infty$, when the electrons are confined to the LLL; the kinetic energy is then an irrelevant constant. Given the extremely large degeneracy in the absence of interactions, it should not come to anyone as a surprise that this problem is not *exactly* solvable. However, as will be seen below, a tremendous insight into its eigenspectrum and the structure of the low-energy eigenstates can be gained based on the single assumption that composite fermions are formed.

5.1. Wave functions of composite fermions

The wave functions of noninteracting composite fermions [6] at ν^* are, as one may guess, related to those of noninteracting electrons at ν^*. In fact, the former are obtained from the latter by attaching $2m$ vortices to each electron, which amounts to multiplication of the noninteracting electron wave function by the Jastrow factor

$$D^m \equiv \prod_{j<k} (z_j - z_k)^{2m}. \tag{11}$$

To see how this factor binds $2m$ vortices to each electron, fix all z_j's except z_1. As z_1 is taken in a closed loop around any other electron, D^m contributes a phase of $4m\pi$, *i.e.*, each electron sees $2m$ vortices on every other electron. (By definition, a closed loop around a unit vortex produces a phase of $\pm 2\pi$.) Denote the many-particle Slater-determinant states of noninteracting electrons at filling factor ν^* by Φ_{ν^*}. This produces

$$\Phi^{\mathrm{CF}}_{\mathrm{unproj},\nu^*} = \prod_{j<k} (z_j - z_k)^{2m} \Phi_{\nu^*} = D^m \Phi_{\nu^*}. \tag{12}$$

This wave function is not restricted to the LLL of electrons, however. Since we will be interested in the $B \to \infty$ limit, we project $\Phi^{\mathrm{CF}}_{\mathrm{unproj}}$ on to the LLL to obtain the wave functions of composite fermions at ν^*, Φ^{CF}, which are

identified with the LLL eigenstates of interacting electrons, χ. This leads to the master equation

$$\chi_\nu = \Phi_{\nu^*}^{\rm CF} = \mathcal{P} \prod_{j<k} (z_j - z_k)^{2m} \Phi_{\nu^*} , \tag{13}$$

or, in shorthand,

$$\chi = \Phi^{\rm CF} = \mathcal{P} D^m \Phi .$$

Here, $\mathcal{P}$ is the LLL projection operator. The right-hand-side of this equation is completely known; it involves the eigenstates of the solvable problem of noninteracting electrons at ν^*. For the special case of $\nu^* = 1$, the ground state wave function of composite fermion is identical to the celebrated Laughlin wave functions [27].

It is possible to see here how the electrons reduce their interaction energy by capturing vortices and turning into composite fermions. Imagine bringing two composite fermions close to one another and denote the distance between them by r. Then, the CF wave function $\Phi_{\rm unproj}^{\rm CF}$ vanishes as a high power of r (as r^{2m+1}) and therefore, the probability of electrons coming very close to one another is small. It must further be assumed that the projection on to the LLL does not destroy these nice correlations built into the CF wave functions. This simple argument, of course, does not *prove* that the nature chooses the CF route, rather than some other more clever way. The validity of the CF theory can be established only from a detailed and careful examination of its consequences both experimentally and theoretically. Our discussion of experiments above leaves little doubt that the CF description is *qualitatively* valid in the range of parameters where the FQHE is observed. Below, we test the CF wave functions *quantitatively.*

The CF wave functions, as the reader may have noticed, contain no fitting parameter, and therefore cannot be improved in any natural way. This lack of a tunable parameter may appear to be a shortcoming of the theory, but actually turns out to be one of the strong points, since, as we will see below, the CF wave functions are extremely accurate as they are.

5.2. Numerical tests

Now we come to a comparison of the CF theory with numerical diagonalization studies. While such studies have the disadvantage that they deal with finite systems of usually fewer than ten electrons, they have the virtue of being exact. Note that the relevant correlation length of the FQHE system is finite due to the presence of a gap, and, in a range of parameters, the numerical systems are already large compared to this length, *i.e.*, effectively thermodynamic.

The CF theory will be compared with numerical calculations at two levels. First is the verification of the qualitative predictions of the theory, and the second concerns the microscopic CF wave functions. Instead of considering several correlation functions, we will simply compute the overlap between the CF wave function and the corresponding Coulomb eigenstate obtained numerically. A near unity overlap will guarantee that all correlation functions as well as the energies of the Coulomb system are well approximated by those of the CF system. All results given below are exact, in the sense that both the Coulomb eigenstates and the CF wave functions are evaluated exactly.

5.3. Spherical geometry

A convenient geometry for the calculations is the spherical geometry [28, 29], which considers N electrons moving on the surface of a sphere under the influence of a radial magnetic field. The flux throught the surface of the sphere, in unit of the flux quantum, is denoted by $2q$, where q is either an integer or a half integer. The eigenstates are labeled by their orbital angular momentum, L. The CF wave functions can be translated into the spherical geometry; the details can be found in Refs [30–32]. The relation between B and B^* is written as

$$q = q^* + m(N-1)\,. \tag{14}$$

The CF theory thus implies that the system of interacting electrons at q resembles that of weakly interacting composite fermions at q^*.

Fig. 4 shows the exact eigenspectrum of eight interacting electrons for several values of q, taken from [33]. Each dash represents a multiplet of $2L+1$ states. It is noteworthy that some multiplets split off from the quasi-continuum to form a low energy band. The number of states in this band and their quantum numbers change from one value of q to another.

Fig. 5 shows the eigenspectrum of eight noninteracting fermions at the corresponding values of q^*. Only the lowest energy states are shown (the other states are separated from these states at least by the cyclotron energy). The reader will notice that these states are in a complete one-to-one correspondence to the low-energy states of interacting electrons in Fig. 4. This has been found to be the case in a large number of studies so far [30–32, 34–36], and demonstrates, in a model independent manner, the formation of composite fermions.

The states in Fig. 5 are uniquely determined by symmetry alone; they do not depend on the form of the interaction. Starting from each state, we construct the CF wave function according to (the spherical version of) Eq. (13), and compute its overlap with the corresponding exact Coulomb eigenstate of Fig. 4. The overlaps are depicted on the Fig. 5 and show that

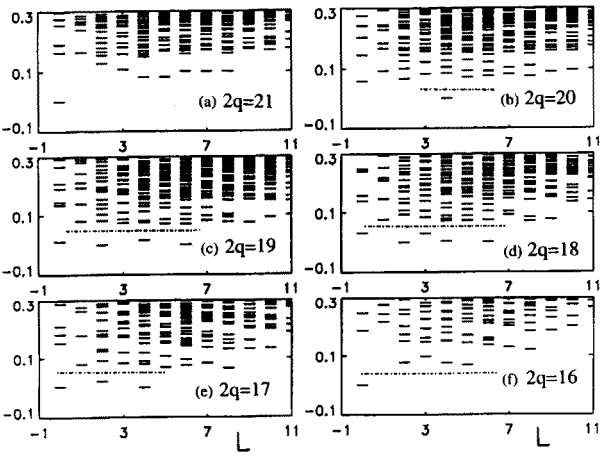

Fig. 4. This figure shows the low-energy spectra of eight interacting electrons on the surface of a sphere at various values of q. The states below the dash-dotted line form the lowest band. The energies are in units of $e^2/\epsilon r_0$ where ϵ is the dielectric constant of the background material and r_0 is the magnetic length. Panel (a) corresponds to $\nu = 1/3$ and (f) to $\nu = 2/5$. Taken from Ref. [33].

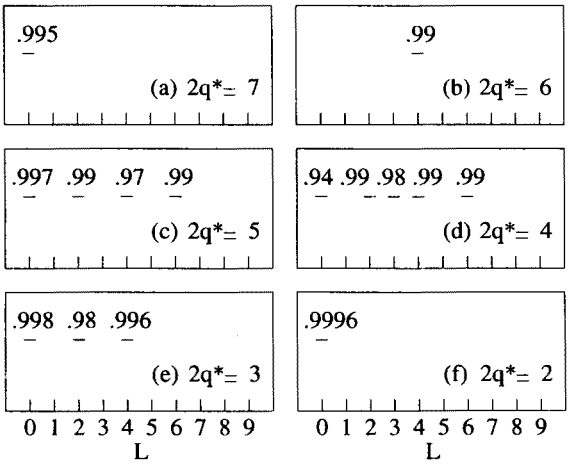

Fig. 5. This figure shows the ground states of eight noninteracting fermions at the values of q^* corresponding to the q of Fig. 4. There is a complete one-to-one correspondence between the lowest bands of Fig. 4 and Fig. 5. The overlaps between the CF states and the corresponding Coulomb states of Fig. 4 are shown on the figure, taken from Ref. [30].

the CF wave functions are almost exact. We emphasize again that the CF wave functions contain no fitting parameters and the Coulomb eigenstates are evaluated without any approximation.

If the composite fermions were completely non-interacting, the low-energy states in Fig. 4 would be degenerate. The amount by which the degeneracy is lifted provides a measure of the residual interaction between the composite fermions. The composite fermions are weakly interacting in the sense that the splitting between the low energy states is small compared to the gap separating them from the other higher energy states.

5.4. Disk geometry

The initial numerical calculations for the FQHE were performed for an electron droplet on a disk [27, 37]. Several downward cusps were observed in the plot of energy as a function of the total angular momentum. However, except for the Laughlin states, it was not clear how to interpret the other states. In particular, it was not known how to assign filling factors to the cusps. This was the main reason why compact geometries, *e.g.* spherical, became more popular. This subsection shows that the CF theory explains the positions of the cusps [38, 39].

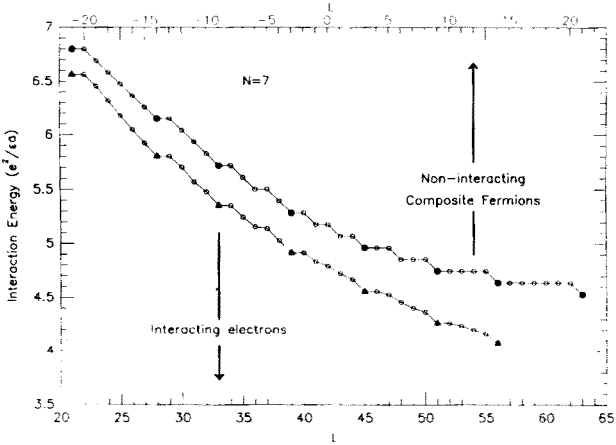

Fig. 6. This figure shows the Coulomb energy of 7 interacting electrons at L, along with the kinetic energy of seven noninteracting composite fermions at $L^* = L - N(N-1)$. The kinetic energy of noninteracting composite fermions at L^* is the same as that of noninteracting electrons at L^*, but with the cyclotron energy of electrons replaced by a suitable effective cyclotron energy of composite fermions. The quantity a is the effective magnetic length depending on the external magnetic field and the confining potential of the quantum dot (it is equal to the magnetic length r_0 in the absence of confinement). The CF curves have been vertically shifted for clarity. Source: Kawamura and Jain, Ref. [42].

In the disk geometry, it is convenient to label states by their total angular momentum. Then,

$$\chi_L = \Phi_{L^*}^{\rm CF} = \mathcal{P} \prod_{j<k} (z_j - z_k)^{2m} \Phi_{L^*}\,, \tag{15}$$

$$L = L^* + mN(N-1)\,, \tag{16}$$

where Φ_{L^*} is the wave function of *noninteracting* electrons with total angular momentum L^*. Any arbitrary L can be related to L^* in the range $-\frac{1}{2}N(N-1) \le L^* < \frac{1}{2}N(N-1)$ with a suitable choice of m.

Fig. 6 plots the kinetic energy of the ground state of noninteracting spinless composite fermions at L^* (which is the same as the kinetic energy of spinless *electrons* at L^*, but with the cyclotron energy replaced by an effective cyclotron energy) and the interaction energy of interacting electrons at L (computed with the LLL restriction). A striking correspondence between the two curves is evident. In particular, all cusps are predicted correctly. The CF wave functions associated with several cusps have been compared with the exact eigenstates, and found to be quite accurate [40, 39].

6. Conclusion

Above we described a model in which the composite fermions are modeled as electrons carrying $2m$ vortices. This suggests wave functions, which were shown to be remarkably accurate. A vortex can often be represented by a magnetic flux quantum, since a loop around a flux quantum also produces a phase (which is the Aharonov-Bohm phase) of 2π. This suggests that the composite fermion can also be thought of as an electron carrying $2m$ flux quanta, which is in fact how they were first envisioned [6]. This model is very conveniently incorporated in a CF-Chern-Simons field theoretical approach [41]. At the mean field level, one obtains fermions moving in a reduced effective magnetic field. Perturbation theory is usually carried out at the RPA level. This approach will be described in the lectures of Prof. Halperin.

In summary, the following picture has emerged. First, electrons form Landau levels due to a quantization of the kinetic energy, producing the IQHE. Within the lowest Landau level, in a broad range of filling factors, electrons find it energetically favorable to transform into composite fermions by capturing an even number of vortices of the wave function. Despite their quantum mechanical, topological and collective character, the composite fermions behave, to a great extent, as ordinary, noninteracting particles moving in an effective magnetic field, producing a number of spectacular effects.

This work was supported in part by the National Science Foundation under Grant No. DMR93-18739. I am indebted to L. Belkhir, G. Dev, A.S. Goldhaber, V.J. Goldman, R.K. Kamilla, T. Kawamura, S.A. Kivelson, D.J. Thouless, N. Trivedi and X.G. Wu for valuable disucussions and collaboration.

REFERENCES

[1] E.H. Hall, *Am. J. Math.* **2**, 287 (1879).
[2] K. von Klitzing, G. Dorda, M. Pepper, *Phys. Rev. Lett.* **45**, 494 (1980).
[3] D.C. Tsui, H.L. Störmer, A.C. Gossard, *Phys. Rev. Lett.* **48**, 1559 (1982).
[4] V.J. Goldman, unpublished.
[5] *The Quantum Hall Effect*, ed. R.E. Prange and S.M. Girvin, Springer-Verlag, Berlin, 1990, 2nd ed.
[6] J.K. Jain, *Phys. Rev. Lett.* **63**, 199 (1989); *Phys. Rev.* **B41**, 7653 (1990); *Science* **266**, 1199 (1994).
[7] A.S. Goldhaber, J.K. Jain, *Phys. Lett.* **A199**, 267 (1995).
[8] J.K. Jain, *Comments Condens. Matter Phys.* **16**, 307 (1993).
[9] See L.D. Landau, E.M. Lifshitz, *Quantum Mechanics*, (2nd ed.) Addison-Wesley, 1965, pp. 424-426.
[10] R.B. Laughlin, *Phys. Rev.* **B23**, 5632 (1981).
[11] J.K. Jain, S.A. Kivelson, N. Trivedi, *Phys. Rev. Lett.* **64**, 1297 (1990).
[12] V.J. Goldman, J.K. Jain, M. Shayegan, *Phys. Rev. Lett.* **65**, 907 (1990); *Mod. Phys. Lett.* **B5**, 479 (1991).
[13] L. Engel, H.P. Wei, D.C. Tsui, M. Shayegan, *Surf. Sci.* **229**, 13 (1990); H.P. Wei, D.C. Tsui, M. Paalanen, A.M.M. Pruisken, *Phys. Rev. Lett.* **61**, 1294 (1988).
[14] L.P. Rokhinson, B. Su, V.J. Goldman, *Solid State Commun.* **96**, 309 (1995).
[15] D.B. Chklovskii, P.A. Lee, *Phys. Rev.* **B48**, 18060 (1993).
[16] N.E. Bonesteel, *Phys. Rev.* **B51**, 9917 (1995).
[17] F.D.M. Haldane, E.H. Rezayi, *Phys. Rev. Lett.* **54**, 237 (1985); R. Morf, B.I. Halperin, *Phys. Rev.* **B33**, 2221 (1986); G. Fano, F. Ortoloni, E. Colombo, *Phys. Rev.* **B34**, 2670 (1986).
[18] B.I. Halperin, P.A. Lee, N. Read, *Phys. Rev.* **B47**, 7312 (1993).
[19] R.R. Du, H.L. Stormer, D.C. Tsui, L.N. Pfeiffer, K.W. West, *Phys. Rev. Lett.* **70**, 2944 (1993). Also see, I.V. Kukushkin, R.J. Haug, K. von Klitzing, K. Ploog, *Phys. Rev. Lett.* **72**, 736 (1994).
[20] D.R. Leadley, R.J. Nicholas, C.T. Foxon, J.J. Harris, *Phys. Rev. Lett.* **72**, 1906 (1994); R.R. Du, H.L. Stormer, D.C. Tsui, L.N. Pfeiffer, K.W. West, *Solid State Commun.* **90**, 71 (1994). For behavior of the effective mass close to $\nu = 1/2$, see: H.C. Manoharan, M. Shayegan, S.J. Klepper, *Phys. Rev. Lett.* **73**, 3270 (1994); R.R. Du, H.L. Stormer, D.C. Tsui, L.N. Pfeiffer, K.W. West, *Phys. Rev. Lett.* **73**, 3274 (1994).
[21] V. Kalmeyer, S.C. Zhang, *Phys. Rev.* **B46**, 9889 (1992).

[22] V.J. Goldman, B. Su, J.K. Jain, *Phys. Rev. Lett.* **72**, 2065 (1994).
[23] W. Kang, H.L. Stormer, L.N. Pfeiffer, K.W. Baldwin, K.W. West, *Phys. Rev. Lett.* **71**, 3850 (1993).
[24] R.L. Willett, R.R. Ruel, K.W. West, L.N. Pfeiffer, *Phys. Rev. Lett.* **71**, 3846 (1993).
[25] G. Kirczenow, B.L. Johnson, preprint.
[26] X. Ying, V. Bayot, M.B. Santos, M. Shayegan, *Phys. Rev.* **B50**, 44969 (1994).
[27] R.B. Laughlin, *Phys. Rev. Lett.* **50**, 1395 (1983).
[28] T.T. Wu, C.N. Yang, *Nucl. Phys.* **B107**, 365 (1976); T.T. Wu, C.N. Yang, *Phys. Rev.* **D16**, 1018 (1977).
[29] F.D.M. Haldane in Ref. [5].
[30] G. Dev J.K. Jain, *Phys. Rev. Lett.* **69**, 2843 (1992).
[31] X.G. Wu, G. Dev, J.K. Jain, *Phys. Rev. Lett.* **71**, 153 (1993).
[32] X.G. Wu, J.K. Jain, *Phys. Rev.* **B51**, 1752 (1995).
[33] S. He, X.C. Xie, F.C. Zhang, *Phys. Rev. Lett.* **68**, 3460 (1992).
[34] M. Kasner, W. Apel, *Phys. Rev.* **B48**, 11435 (1993); U. Girlich, M. Hellmund, *Phys. Rev.* **B49**, 17488 (1994).
[35] E.H. Rezayi, A.H. MacDonald, *Phys. Rev.* **B44**, 8395 (1991).
[36] E.H. Rezayi, N. Read, *Phys. Rev. Lett.* **72**, 900 (1994); J. Yang, *Phys. Rev.* **B50**, 8028 (1994).
[37] D.J. Yoshioka, B.I. Halperin, P.A. Lee, *Phys. Rev. Lett.* **50**, 1219 (1983); S.M. Girvin, T. Jach, *Phys. Rev.* **B28**, 4506 (1983).
[38] B. Rejaei, *Phys. Rev.* **B48**, 18016 (1993); C.W.J. Beenakker, B. Rejaei, *Physica* **B189**, 147 (1993).
[39] T. Kawamura, J.K. Jain, *J. Phys. Condens. Matter*, in print; J.K. Jain, T. Kawamura, *Europhys. Lett.* **29**, 321 (1995); R.K. Kamilla, J.K. Jain, *Phys. Rev.* **B52**, 2798 (1995).
[40] G. Dev, J.K. Jain, *Phys. Rev.* **B45**, 1223 (1992).
[41] A. Lopez, E. Fradkin, *Phys. Rev.* **B44**, 5246 (1991).